Supplementary Information

The configuration entropy ($\Delta S_{\mathrm{config}}$) of these ceramics can be calculated according to the following equation:

$$\Delta S_{\mathrm{config}} = -R\left[\left(\sum_{a=1}^{n} x_a \ln x_a\right)_{A-site} + \left(\sum_{b=1}^{n} x_b \ln x_b\right)_{B-site} + 3\left(\sum_{c=1}^{n} x_c\, ln x_c\right)_{O-site}\right] \text{* MERGEFORMAT (1)}$$

where R is the ideal gas constant (R = 8.314 J/mol·K), and x_{a}, x_{b}, and x_{c} represent the molar ratios of A-site, B-site, and O-site ions, respectively. When $\Delta S_{\mathrm{config}}$ > 1.61R, the materials are classified as high-entropy materials. Therefore, $\Delta S_{\mathrm{config}}$ gradually increases over a wide range from 1.48 R to 1.77 R, as shown in Table S1.

Table S1 $\Delta S_{\mathrm{config}}$ values for $0.85Bi_{0.35}Na_{0.35}Sr_{0.3}TiO_3$-$0.15K_xNa_{(1-x)}NbO_3$ (x = 0, 0.25, 0.5, 0.75, 1) ceramics.

Compositions	$\Delta S_{\mathrm{config}}$ (R)
$x = 0$	1.48
$x = 0.25$	1.61
$x = 0.5$	1.69
$x = 0.75$	1.74
$x = 1$	1.77

Table S2 The structural parameters of XRD Rietveld refinement with different $\Delta S_{\mathrm{config}}$ ceramics.

$\Delta S_{\mathrm{config}}$ (R)	Space group	a/Å	c/Å	a/deg	Volume/Å^3
1.48	*R3c*	5.523	13.530	90	357.510
	P4bm	5.524	3.911	90	119.387
1.61	*R3c*	5.527	13.540	90	358.285
	P4bm	5.530	3.911	90	119.660
1.69	*R3c*	5.536	13.561	90	359.961
	P4bm	5.545	3.936	90	121.025
1.74	*R3c*	5.543	13.579	90	361.434
	P4bm	5.570	3.961	90	122.885
1.77	*R3c*	5.554	13.580	90	362.818
	P4bm	5.575	3.967	90	123.320

Table S3 XRD refinement results for the 1.77R sample: Partial crystal plane spacings (*d* values) between the R phase and T phase

No.	R phase crystal plane index (hkl)	R phase crystal plane spacing *d* (nm)	T phase crystal plane index (hkl)	T phase crystal plane spacing *d* (nm)
1	1 1 0	0.276	1 1 1	0.277
2	1 0 4	0.276	0 0 1	0.393
3	1 0 -2	0.391	1 1 0	0.392

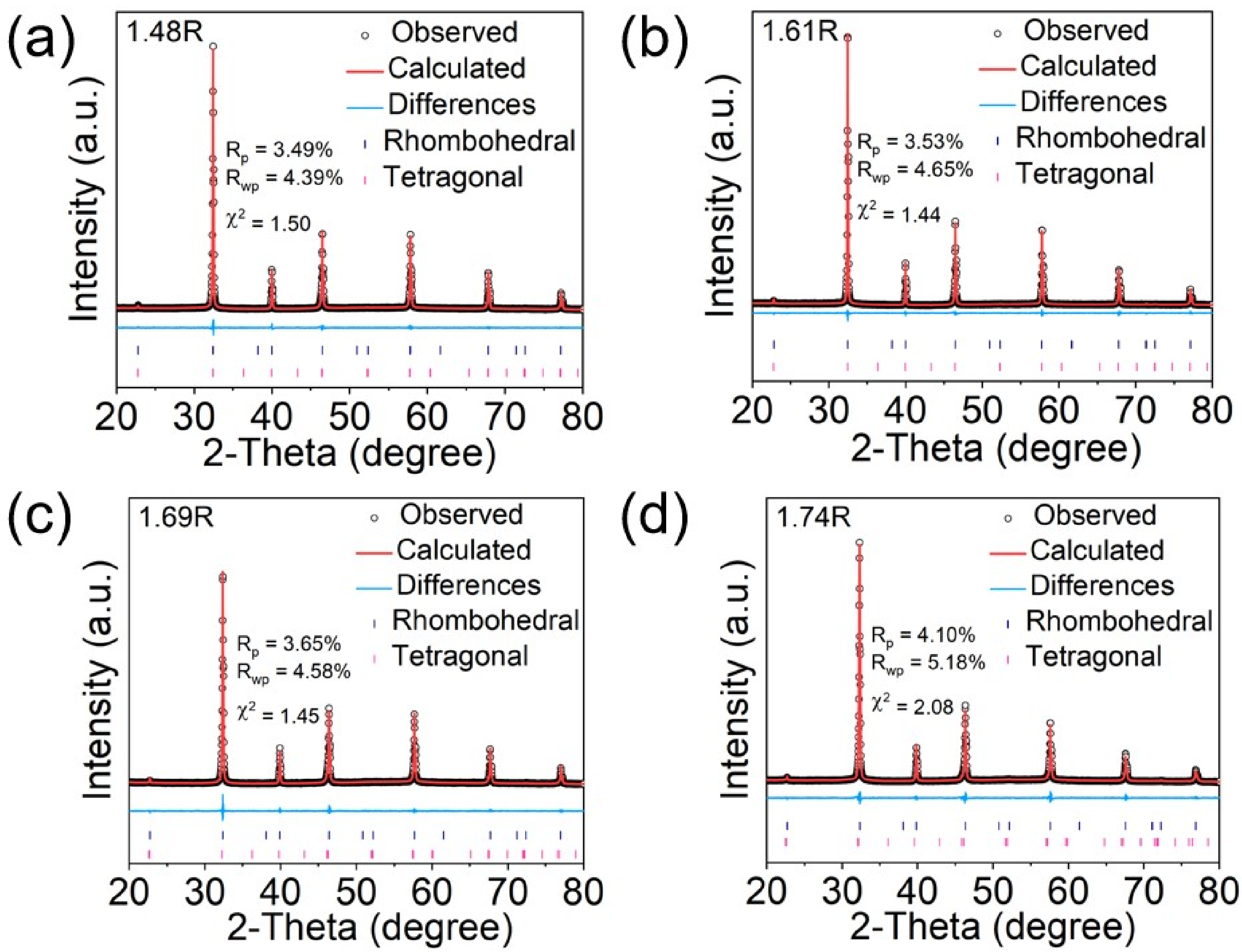

Fig. S1. Rietveld refinement results of XRD data of (a) 1.48R, (b) 1.61R, (c) 1.69R and (d) 1.74R samples.

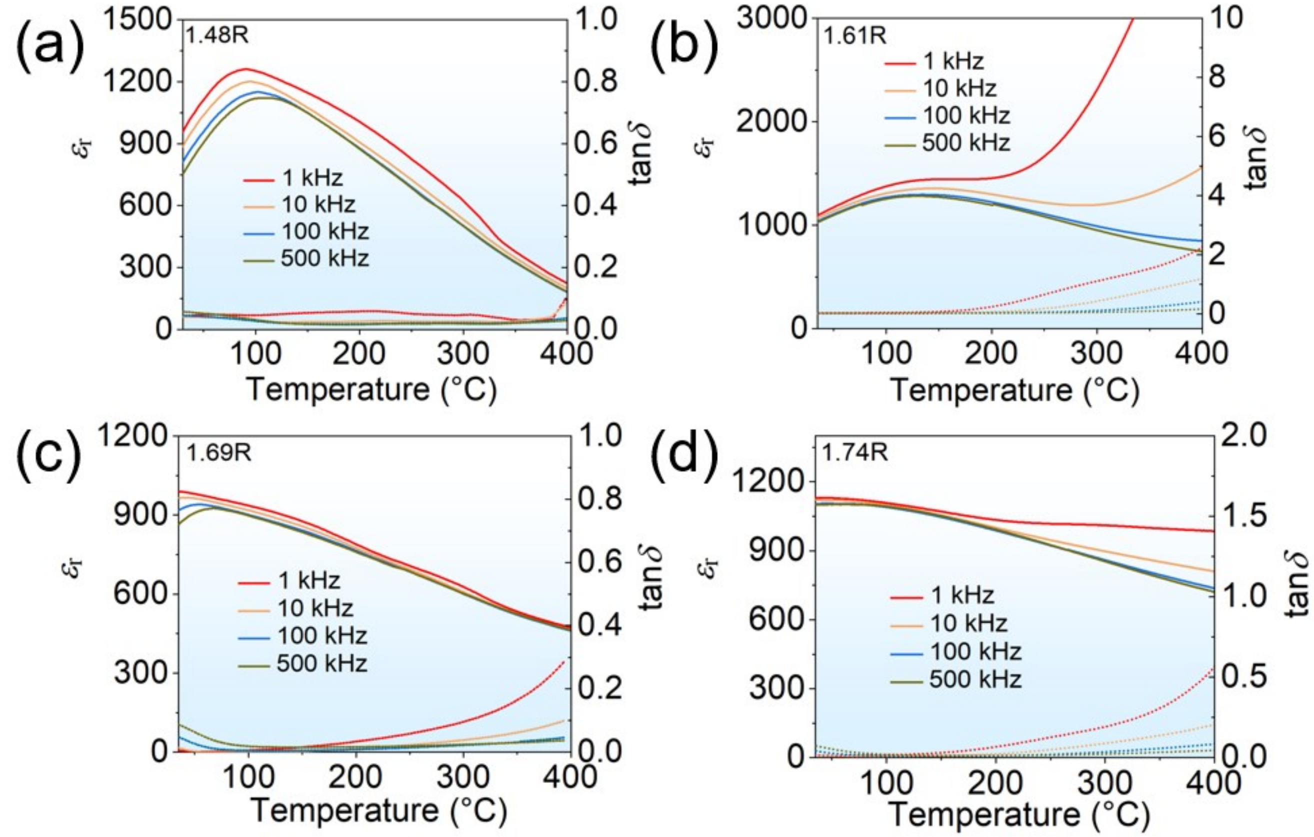

Fig. S2. Dielectric temperature spectrum of 1 kHz, 10 kHz, 100 kHz and 500 kHz for (a) 1.48R, (b) 1.61R, (c) 1.69R and (d) 1.74R ceramic samples.

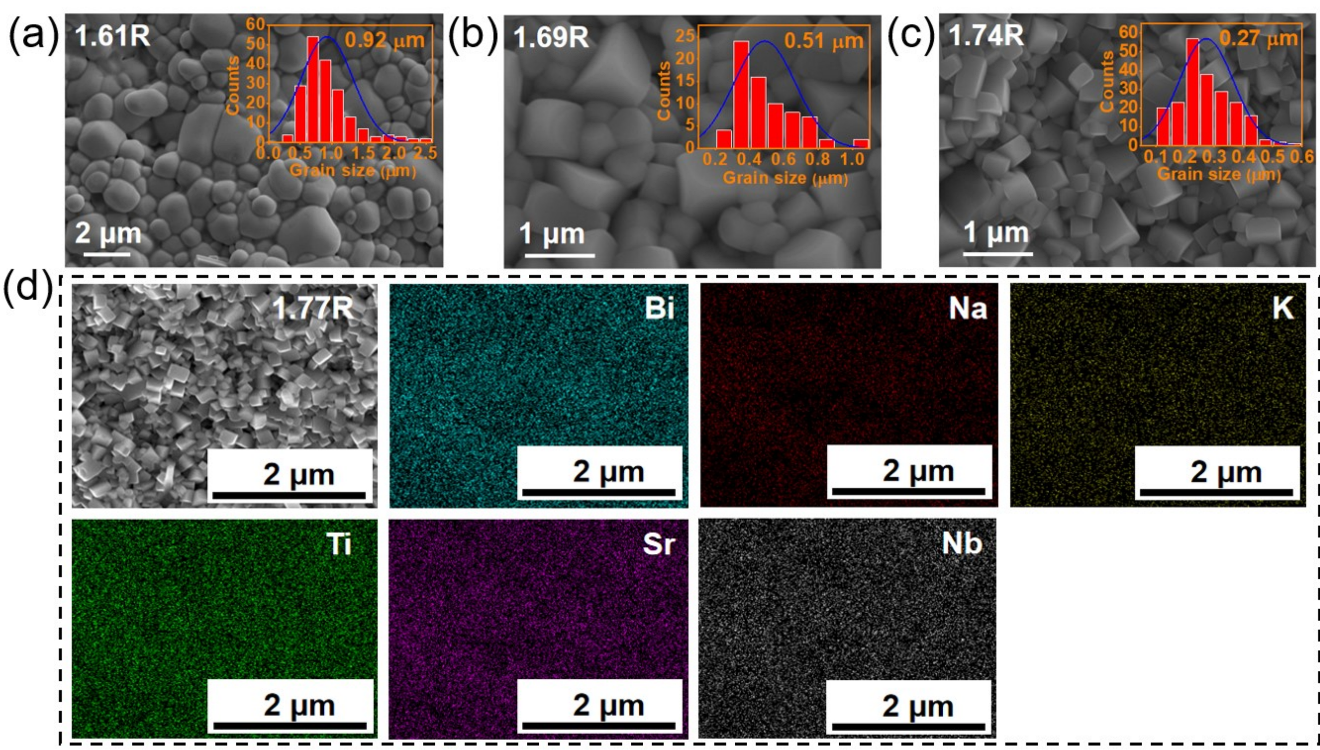

Fig. S3. SEM images and size distribution histograms of ceramics: (a) 1.48R, (b) 1.61R, (c) 1.69R. (d) EDS mapping images of the ΔS_{config} = 1.77R ceramics.

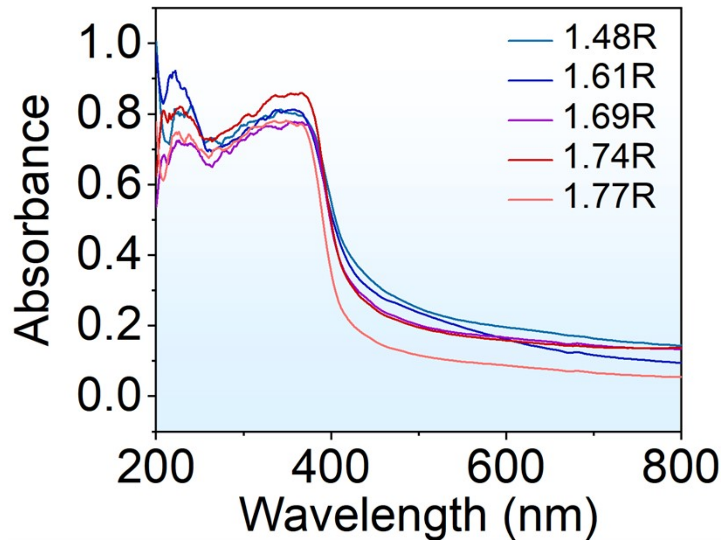

Fig. S4. UV-Vis absorbance curves of different ceramics

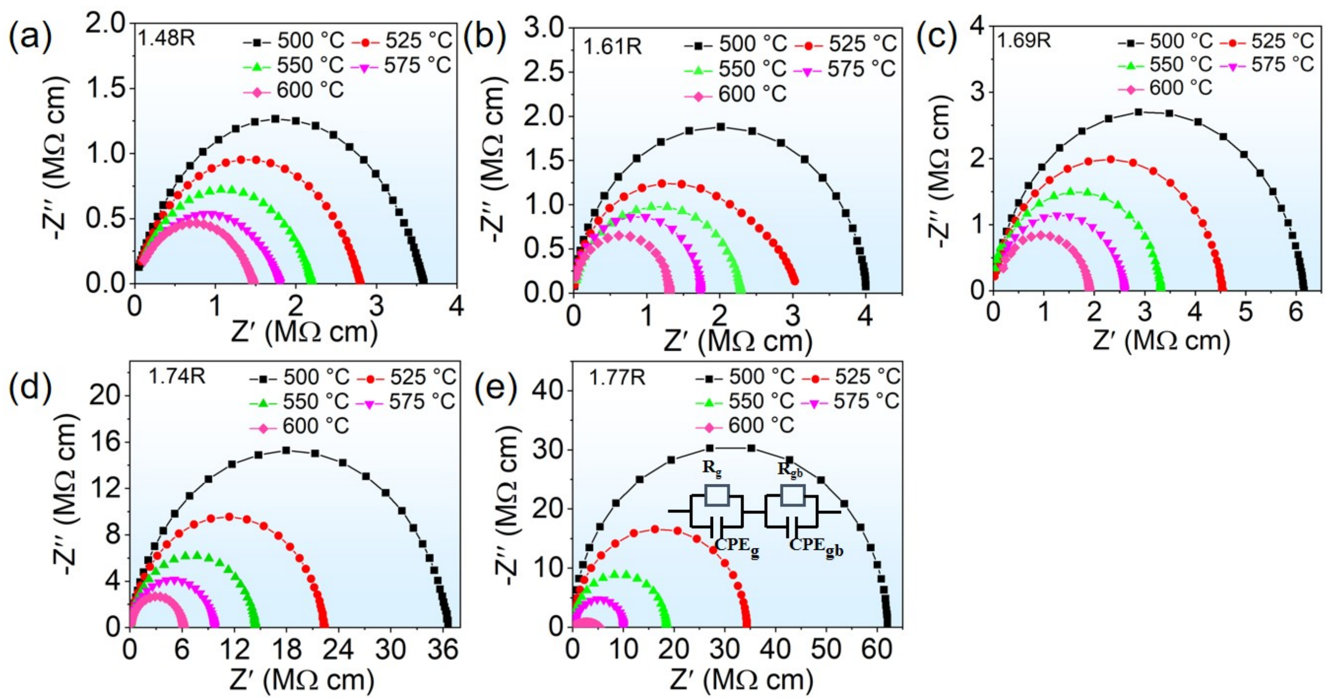

Fig. S5. The impedance spectroscopy at various temperatures of (a) 1.48R, (b) 1.61R, (c) 1.69R, (d) 1.74R, and (e) 1.77R ceramics.

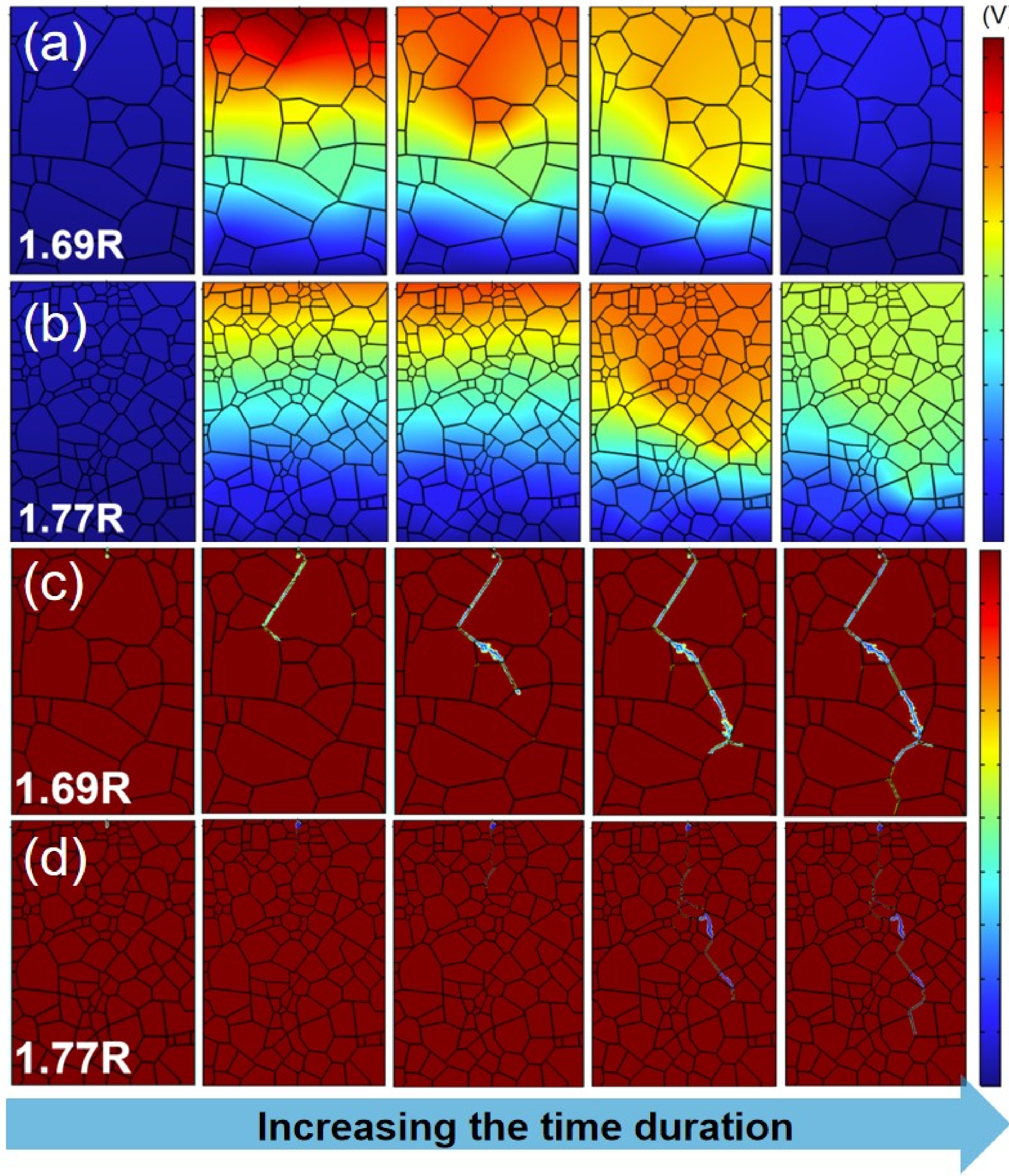

Fig. S6. The breakdown path distribution and electrical tree evolution of ceramics of (a) 1.69R and (b) 1.77R. Potential distribution of ceramic of (c) 1.69R and (d) 1.77R.

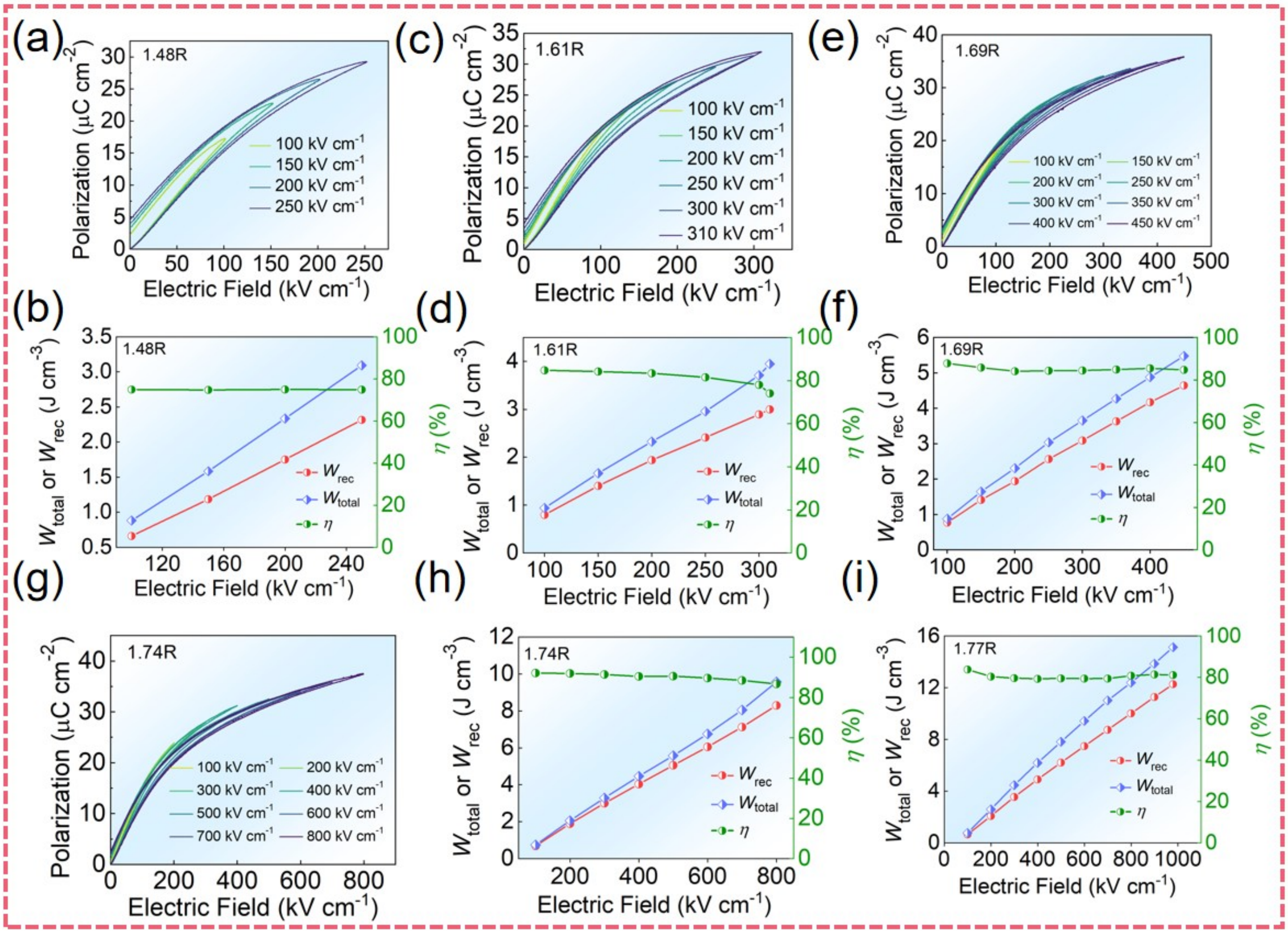

Fig. S7. (a-b) 1.48R, (c-d) 1.61R, (e-f) 1.69R, (g-h) 1.74R, and (i) 1.77R unipolar *P-E* loops and energy storage properties of ceramics from low field to E_b.

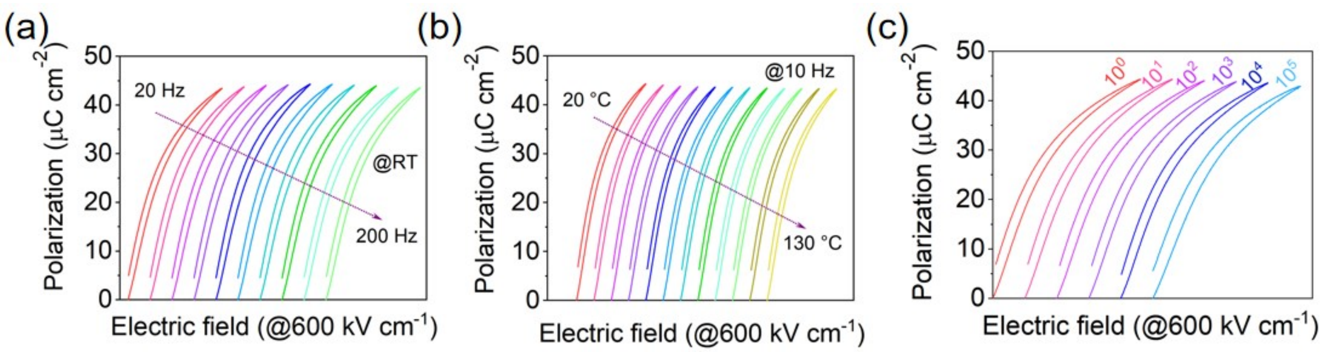

Fig. S8. Unipolar *P-E* loops from (a) 20 Hz to 200 Hz, (b) 20 °C to 200 °C and (c) 10^0 to 10^5 cycles under the 600 kV cm^{-1}.